EDGE ARTICLE

Check for updates

Host–guest interaction-induced selective oxidation of a substrate inside an aqueous Pd₆L₄ cage

Shamsad Ali, Debsena Chakraborty and Partha Sarathi Mukherjee [ID] *

Chemical transformations inside artificial hosts like cages have been a booming field of research. However, the use of such artificial hosts for carrying out the selective transformation of one molecule from a mixture of different molecules has been underexplored. Herein, we report the oxidation of the benzylic $C(sp^3)$–H of alkylarenes inside an aqueous Pd₆L₄ cage **1** without using any traditional oxidant. **1** was an efficient host in inducing complete oxidation of alkyl arenes such as xanthene, thioxanthene, fluorene, and acridine derivatives inside its cavity, which other reported analogous Pd₆ cages did not show under similar conditions. It was also observed that encapsulation within the cage was a necessary criterion for oxidation to occur in water. Using this criterion and the higher binding affinity of cage **1** to fluorene over other fluorene derivatives such as 2-bromofluorene and 2,7-dibromofluorene, **1** was able to selectively oxidize fluorene from a mixture of fluorene derivatives through selective encapsulation. This work provides insight into an alternative approach for the selective oxidation of active methylene-containing organic compounds using differences in host–guest affinity in an aqueous environment.

Introduction

In nature, enzymes function as molecular containers, featuring pockets that enable substrates to bind through non-covalent interactions, facilitating numerous chemical reactions.[1] The interactions between such enzymes and substrates are highly specific owing to the presence of multiple non-covalent interactions between the substrate and the enzyme.[2] Such highly specific interactions enable enzymes to catalyse the reactions of only certain substrates from a milieu of different compounds.[3] Over recent decades, chemists have created a diverse range of artificial hosts that mimic enzyme-like capabilities and have a variety of shapes, sizes, and functions.[4–6] These artificial structures, containing well-defined internal cavities, are often referred to as host molecules, while the entities they encapsulate are called guest molecules. Hosts can be classified as either organic or metal–organic.[7–11] Organic cages, which are neutral, self-assembled structures, dissolve in organic solvents but often exhibit weaker guest binding abilities. Consequently, organic cages and macrocycles have seen limited application in catalysing chemical transformations within their cavities in aqueous medium.[12–14] Conversely, metal–organic cages provide notable advantages due to their charged nature, enhancing their solubility in polar solvents such as water.[15–18] These water-soluble hosts are generally synthesized *via* coordination-driven self-assembly, where metal acceptors and donor ligands form

thermodynamically stable three-dimensional (3D) structures in a single step.[19] This metal–ligand self-assembly process is a highly efficient method for constructing intricate molecular architectures.[20–22] In aqueous environments, metal–organic cages exhibit strong binding to organic guest molecules, which typically have little to no solubility in water. The hydrophobic cavities within these cages promote tight binding through hydrophobic interactions. Additionally, host–guest complexes are stabilized by various non-covalent interactions, such as π–π interactions, hydrogen bonding, CH–π interactions, and van der Waals forces. These characteristics make metal–organic cages particularly promising for applications in light harvesting,[23–25] sensing,[26,27] separations,[28,29] and stabilizing transient species.[30,31]

Much like enzymes, cages are also capable of acting as hosts for carrying out chemical transformations inside their cavities. Different chemical reactions have been demonstrated inside cages ranging from Knoevenagel condensation,[32] Diels–Alder reaction[33] to aza-Darzens reaction[34] and many more.[35–39] Such chemical transformations differ from traditional reactions in one key aspect: in the case of the former, host–guest interactions play a crucial role in determining the outcome of the final product.[40,41] In traditional chemical reactions, selectivity often arises from differences in reactivity, where the more reactive substrate reacts faster, and under limiting conditions, the less reactive ones can remain unreacted.[42,43] The measure of reactivity often comes down to differences in bond dissociation energies and/or the electrophilicity of the reacting groups and other non-covalent factors seldom play a significant role.

Department of Inorganic and Physical Chemistry, Indian Institute of Science, Bangalore-560012, India. E-mail: psm@iisc.ac.in
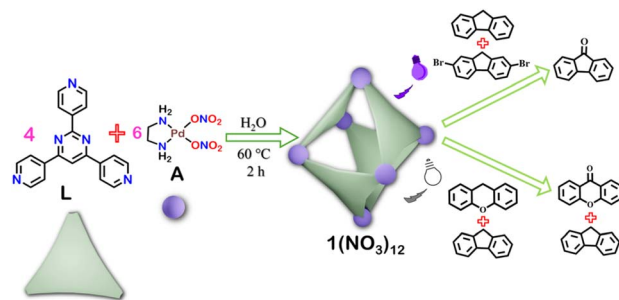
Scheme 1 Schematic representation of the cage synthesis and the selective oxidation reaction.

However, when it comes to reactions inside cages, the non-covalent interactions between the encapsulated substrate and the cage and by extension their association constants play a crucial role.[44–46] Thus, the question arises: can we take different substrates with different binding efficiencies to the host molecule and achieve selective chemical transformation of one substrate over another? Interestingly, the ability of cages to selectively bind certain molecules has been used for separation of isomers[29,30] but its utility for selective chemical transformation inside cages has been limited. Most examples of selective reactions have been demonstrated only in terms of Diels–Alder reactions[47,48] and the utility of such cages in carrying out selective chemical transformation in terms of other chemical reactions such as oxidation reactions remains underexplored. Furthermore, to the best of our knowledge, selectivity between substrates that otherwise undergo facile oxidation inside a cage has not been demonstrated before.

Herein, we report the selective oxidation of fluorene derivatives inside a newly synthesised water-soluble cage 1. Cage 1 was synthesized through the metal–ligand-coordination-driven self-assembly of the pyrimidine-based tripyridyl ligand with 90° cis-blocked Pd^{II} acceptor A (Scheme 1). The optimized structure of 1 showed the presence of a large cavity capable of encapsulating various organic guest molecules. The capability of 1 to encapsulate a variety of planar and non-planar guest molecules in water was investigated. Inside the cavity of cage 1, xanthene (9H-xanthene) and similar molecules underwent facile oxidation to form oxidized products without using traditional oxidants. The same reaction was then performed inside different cages with the same stoichiometry (A_6L_4) and it was found that the reaction was fastest inside cage 1. It was also observed that the formation of the host–guest complex was a crucial criterion for the oxidation of the guest molecule. The selective host–guest binding ability of the cage was then utilized for the selective oxidation of fluorene over 2,7-dibromofluorene with a selectivity of >99% and over 2-bromofluorene with a selectivity of 84%. To the best of our knowledge, this is the first example of host–guest interaction-based selective oxidation of substrates.

Results and discussion

Synthesis and characterization

The pyrimidine-based tripyridyl ligand L was synthesized as per a previously reported procedure,[49] by the base-mediated condensation of 4-acetylpyridine and 4-pyridinecarbonitrile at 120 °C in an autoclave reactor (Scheme S1). The ligand was characterized by ESI-MS, ^{1}H, and ^{13}C NMR in CDCl$_3$ (Fig. S1–S3). The ligand L exhibited a 2:1 splitting of the α- and β-hydrogens of the pyridine rings owing to its asymmetric characterisics (Fig. 1 and S1). The signals are designated as a and a′ for the α-hydrogens of the pyridine rings and b and b′ for the β-hydrogens of the pyridine rings of L.

1 was synthesized by the self-assembly of L with cis-[(en)Pd(NO$_3$)$_2$] (A) [en = ethylenediamine] in a 2:3 molar ratio in water at 60 °C for 2 hours (Scheme S2). The solution became transparent during the reaction as the ligand was consumed. After the reaction was completed, 1 was obtained by concentrating the solution under reduced pressure and triturating it with acetone.

The analysis of 1 was conducted using ^{1}H NMR (in D$_2$O), revealing three unique peaks in the aromatic region (Fig. 1 and S4). ^{1}H DOSY analysis indicated that all three peaks correspond to the same assembly, with a shared diffusion coefficient of $D = 1.62 \times 10^{-10}$ m^2 s^{-1} (log $D = -9.79$) and the hydrodynamic radius r_h is 12.17 Å. The peaks were additionally analysed using ^{1}H–^{1}H COSY and NOESY NMR in D$_2$O (Fig. S6 and S7). From COSY and NOESY data, we found that the α-hydrogen peaks (a and a′) of the pyridine rings (which were separate in ligand L) were merged in the ^{1}H NMR of the self-assembled cage. Additionally, one of the β-hydrogen peaks (designated as b) coincided with the pyrimidine peak (designated as c). This led to a smaller number of peaks in the ^{1}H NMR of the self-assembled cage compared to that of ligand L. The proton integration of 1 was subsequently verified (Fig. S4). Owing to the low symmetric nature of the ligand L, the self-assembled cage could have the ligands arranged in different ways such that the central
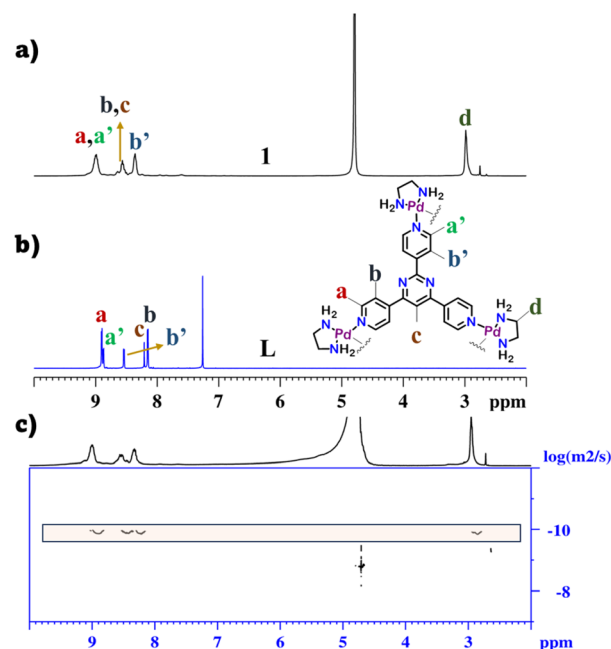

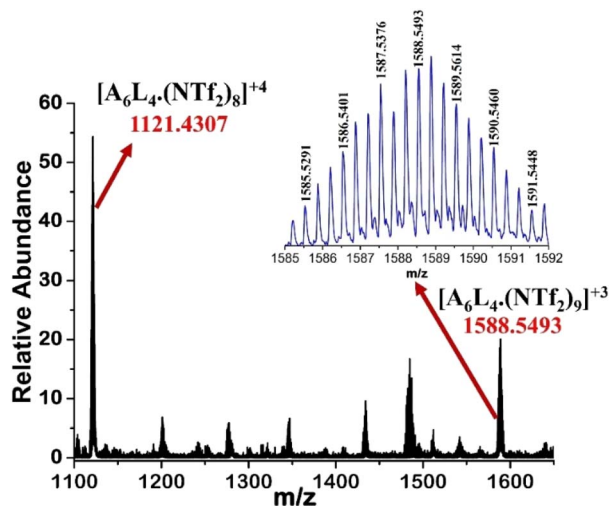Fig. 1 Stacked ^{1}H NMR spectra of (a) cage 1 in D$_2$O and (b) ligand L in CDCl$_3$, and (c) ^{1}H NMR DOSY spectrum of 1 in D$_2$O.

Fig. 2 ESI-MS spectrum of the NTf_2^- analogue of **1** in acetonitrile. The experimental isotopic distribution pattern of the $[A_6L_4(NTf_2)_9]^{3+}$ fragment (inset).

pyrimidine core could orient itself in different positions, and this led to an overall broadening of the ^1H NMR peaks of cage **1**.

To determine the composition of the cage, the ESI-MS spectrum of the NTf_2^- analogue was recorded in acetonitrile. The spectrum showed peaks at $m/z = 1121.4307$ and 1588.5493, corresponding to the fragments $[A_6L_4(NTf_2)_9]^{3+}$ and $[A_6L_4(NTf_2)_8]^{4+}$ (Fig. 2 and S8). It showed that **1** was a [6 + 4] self-assembly of the acceptor **A** with the tridentate ligand **L**. Such self-assembled products can either have a double-square[50] or an octahedral shape.[51] In double-square structures, ligand peaks split in a 1 : 2 ratio; as this splitting was not observed in the ^1H NMR of cage **1**, it could thus be concluded that **1** possessed an

octahedral structure. However, after several attempts, single crystals of **1** suitable for X-ray diffraction could not be obtained. The structure of **1** was thus optimized using the DFT method and the LanL2DZ basis set was used in the case of the palladium atom and the 6-31g(d) basis set for all other atoms in all calculations.

1 was optimized in the octahedral structure. This showed that an octahedral structure would have a distance of 18.7 Å between diagonally positioned Pd atoms and 12.9 Å between adjacent Pd atoms (Fig. 3). As such a large cavity would suggest that **1** could encapsulate different smaller guests, the capability of **1** to encapsulate a variety of organic molecules like pyrene, xanthene, fluorene, thioxanthene, and acridine derivatives was investigated.

Guest encapsulation studies

The host–guest chemistry of **1** was investigated with xanthene, thioxanthene, fluorene, acridine, and their derivatives. Excess solid xanthene (**X**) was introduced into an aqueous solution of **1** to evaluate the guest encapsulation capabilities, and the mixture was heated at 50 °C for 10 hours. A yellow turbid was formed, which was subsequently centrifuged, and the supernatant was utilized for further characterization. The ^1H NMR of this solution (termed as **X⊂1**) exhibited additional peaks in the upfield area of 7 ppm (Fig. 4 and S9). Correspondingly, the α-hydrogen peaks of the pyridine rings exhibited a downfield shift. The alteration in the ^1H NMR peaks of the host and guest molecules indicated the encapsulation of the guest within the cavity of a cage. The internal binding was additionally confirmed by the ^1H DOSY NMR of **X⊂1** in D_2O, which exhibited a single diffusion band $[D = 1.26 \times 10^{-10}\ m^2\ s^{-1}$ ($\log\ D = -9.9$)] (Fig. S10). The host–guest interaction was corroborated by the ^1H–^1H NOESY NMR study of **X⊂1** in D_2O. This demonstrated a correlation between the α-hydrogens of the pyridine rings of **1** and the upfield-shifted aromatic protons of **X** (Fig. S11).
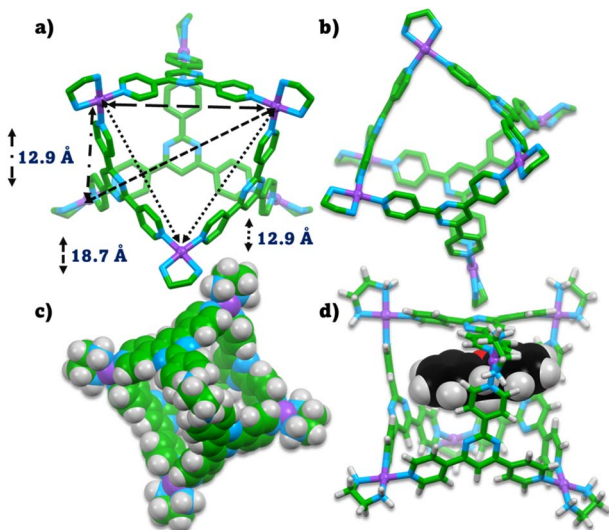

Fig. 3 The DFT optimized structure of **1**. (a) view of the inner cavity with different Pd–Pd distances labelled, (b) side view of **1**, (c) space-fill model of **1** [color scheme: H, white; C, green; N, blue; Pd, purple], and (d) the PM6 optimized structure of the host–guest complex with the space-fill model of the guest inside the cavity of **1**.
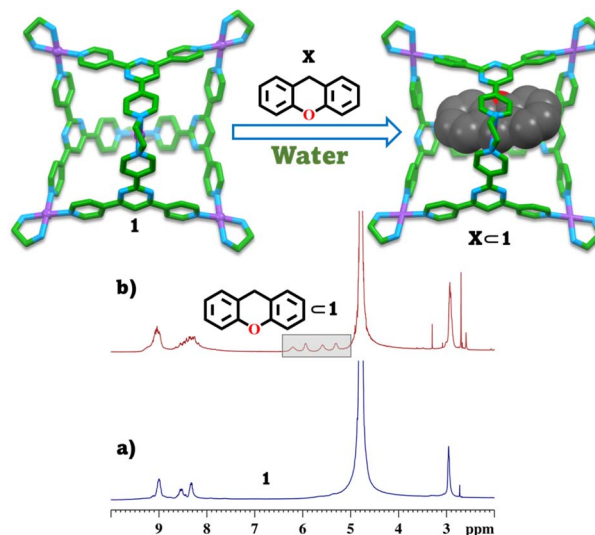

Fig. 4 ^1H NMR stack plot of (a) **1** in D_2O, (b) **X⊂1** (**X**: xanthene) in D_2O. The guest peaks are highlighted in grey.

Oxidation of guests in aqueous medium through encapsulation inside cage 1

As cage **1** could encapsulate a variety of guests, its ability to act as a host for chemical reactions was investigated. The facile oxidation of xanthene, thioxanthene, fluorene, acridine, and their derivatives was studied under confinement inside cage **1**. The reaction was selected as these oxidized guest molecules hold significant importance due to their diverse biological activities and practical applications. Specifically, xanthones (the oxidized form of xanthene) have been utilized to treat various diseases, including convulsions, hypertension, thrombosis, tumours, and Alzheimer's disease.[52–55] Similarly, thioxanthone derivatives find extensive use in microelectronics, coatings, photoresists, and photo-initiators.[56–59]

Acridones also play a vital role in medicine, particularly due to their substantial antitumor activity.[60,61] It has been reported that the oxidation of such compounds can be performed under mild conditions in organic solvents like DMSO;[62] however, a report of the reaction in aqueous medium is not known.

The reaction was first performed with xanthene (**X**) as the model compound. To an aqueous solution of **1**, solid **X** (5 mg, excess) was added and stirred at 50 °C for 10 h. The resultant solution was then centrifuged and a clear supernatant that contained the aqueous solution of the host–guest complex **X⊂1** was collected. The solution was then stirred in the presence of white light [45 W LED ($\lambda > 400$ nm)] at 50 °C for 10 hours. The product obtained was then extracted with chloroform and analyzed by ^{1}H NMR and ESI-MS. The aqueous solution of the cage (after removal of the product) could then be further used for another set of reactions (Scheme S4). The ^{1}H NMR and ESI-MS of the product showed that under these conditions xanthene was oxidized to xanthone (**XO**) with >96% conversion.

The reaction of xanthene was optimized by performing the reaction under different conditions (Table 1). In the presence of TEMPO [(2,2,6,6-tetr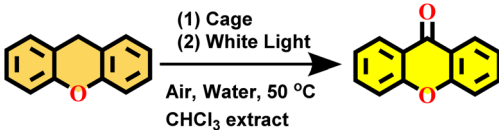amethylpiperidin-1-yl)oxyl], a recognized radical scavenger, the reaction involving **1** yielded a reduced amount of **XO** (Table 1 and Fig. S33). This analysis verified that the reactions within **1** transpired through the generation of a radical species. In this regard, the adduct of TEMPO with the intermediate radical species was trapped and characterized by ESI-MS (Fig. S34).

It was further observed that the reaction inside cage **1** occurred even under an argon (Ar) inert atmosphere (Table 1 and Fig. S33). However, if the reaction was done in a non-aqueous solvent like acetonitrile, the product was not formed. This suggests that H_2O (solvent) could in the absence of oxygen act as an oxidizing agent for the formation of **XO**. Similar unusual oxidation of molecules inside cages by H_2O has been previously reported.[63] In the cage, the radical can react with molecular oxygen or, in its absence, with H_2O to produce the oxidized product.

Interestingly, the ligand and acceptor did not show any significant oxidation of xanthene (Fig. S33), which clearly showed that encapsulation was pivotal for oxidation to occur in aqueous medium. Similarly, in the absence of cage **1**, only xanthene in aqueous medium remained unoxidized when subjected to similar conditions (Fig. S33). Based on these findings, a mechanism could be envisioned (Fig. S31a), which followed previously known mechanisms for oxidation inside cages.[64,65] After light irradiation, a radical was generated on the benzylic carbon of the guest molecule and subsequently this radical was rapidly trapped by oxygen or water (in the absence of O_2) to yield the oxidized product. Inside the host **1**, only one molecule of the xanthene was encapsulated as shown by the ^{1}H NMR integration (Fig. S13), which ruled out any possibility of dimerization of the xanthene radical and only the oxidized product was obtained.

Next, we wanted to study the utility of cage **1** in oxidizing the substrate compared to other previously known cages. Thus, oxidation of xanthene inside cages **2** and **3** was explored under

Table 1 Conditions for the reaction performed with **1**. The percent conversion was calculated using ^{1}H NMR, based on the relative abundance of the product (**XO**) peaks in the CHCl$_3$ extract from the aqueous solution after the reaction *versus* that of the starting material (**X**) peaks, and % conversion was calculated by ^{1}H NMR using 1,3,5-trimethoxybenzene as an internal standard

Entry	Solvent	Atmosphere	Temperature	Light	Time	Cage/acceptor/ligand	Conversion
1	Water	Air	r. t.	Yes	10 h	Cage	70%
2	**Water**	**Air**	**50°C**	**Yes**	**10 h**	**Cage**	**>96%**
3	Water	Air	50 °C	Yes	10 h	Ligand	No reaction
4	Water	Air	50 °C	Yes	10 h	Acceptor	No reaction
5	Water	Argon	50 °C	Yes	10 h	Cage	95%
6	Water	Air	50 °C	No	10 h	Cage	30%
7	CH$_3$CN	N$_2$	50 °C	Yes	10 h	Cage	10%
8	Water	Air	50 °C	Yes	10 h	Blank	No reaction
9	Water/CH$_3$OH	Air	50 °C	Yes	10 h	Blank	No reaction
10	Water + TEMPO	Air	50 °C	Yes	10 h	Cage	42%

the same reaction conditions (Fig. 5). **2** has a similar octahedral structure to **1**, while **3** has a double-square structure. It was observed that within the same time frame, complete oxidation of xanthene was not possible inside cages **2** and **3** and the product formed contained a higher amount of unreacted xanthene (45% and 35% for cages **2** and **3**, respectively) along with the oxidized product xanthone (**XO**). To understand the reason behind this, we monitored the product formation inside different cages by ¹H NMR. It could be seen that product formation inside cage **1** was faster than inside cages **2** and **3** (Fig. S31b), probably due to better binding of the guest and reactive intermediate species inside cage **1** compared to the other cages (**2** and **3**) (Table S1). The profile obtained for the % conversion *vs.* time graph was complicated and further conclusions could not be drawn in part due to the experimental limitations and the complicated nature of the reaction mechanism, which involves multiple reaction intermediates (Fig. S31b). However, the faster product formation inside cage **1** and the usefulness of this cage over other cages (**2** and **3**) could be clearly demonstrated.

Next the usefulness of this oxidation procedure to oxidize other substrates was investigated. Thioxanthene and acridine derivatives could also be oxidized in a similar fashion (Fig. 6). However, in the case of fluorene and its derivatives, owing to a higher C–H bond strength as compared to xanthene and acridine derivatives, greater activation energy was required. Thus, a 390 nm 100 W LED was required instead of white light for 10 hours at ambient temperature, to efficiently oxidize fluorene and its derivatives.
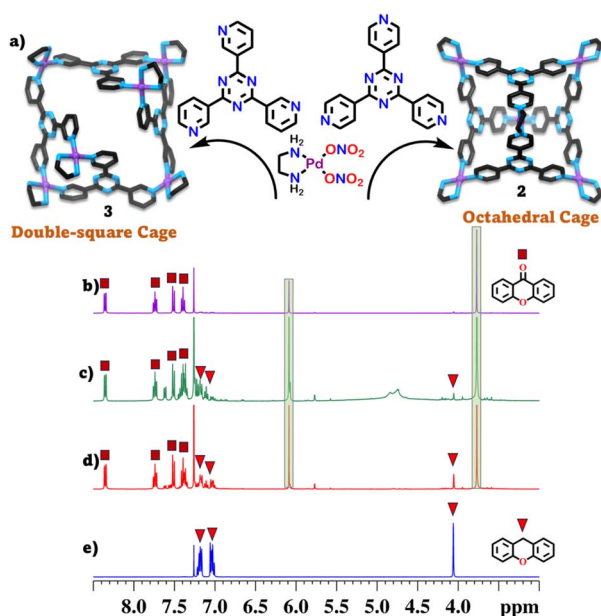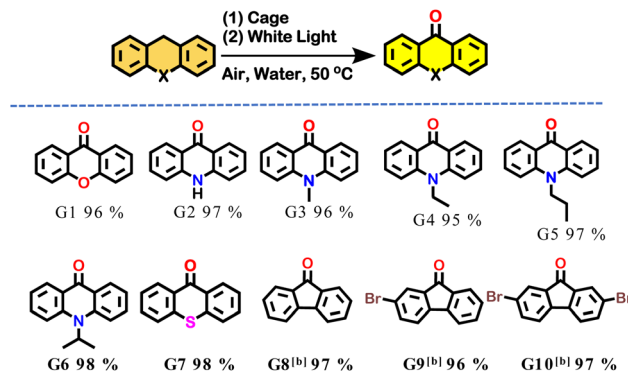

Fig. 6 Scope of the aqueous cage **1** catalyzed C(sp³)–H oxidation of alkylarenes. The yield is calculated by ¹H NMR using 1,3,5-trimethoxybenzene as an internal standard [b: a 390 nm 100 W LED was used]. The % conversion was calculated by ¹H NMR using the internal standard 1,3,5-trimethoxybenzene.

Selective oxidation using cage 1

In the literature, most transition metal catalysts use the difference in reactivity of substrates to achieve selectivity. In the case of cage **1**, this can be easily achieved with a mixture of xanthene and fluorene. As the C–H bond strength of fluorene is stronger than that of xanthene, if we take an equimolar mixture of xanthene and fluorene and treat it with an aqueous solution of cage **1** and subject it to white light irradiation at 50 °C for 10 hours (following the optimized procedure in Scheme S4), only xanthene could be oxidized selectively (Fig. 7c). The ¹H NMR of the product showed peaks for xanthone and unoxidized fluorene. However, we wanted to investigate the possibility of selective oxidation through host–guest chemistry using non-covalent interactions.

To examine this, we chose fluorene and its derivatives. First, a mixture of fluorene and 2,7-dibromofluorene was selected. An equimolar ratio of the two was added to an aqueous solution of **1** and then the mixture was stirred for 12 hours at 60 °C. The same reaction mixture was irradiated under a 390 nm LED at room temperature for 10 hours. The mixture was then centrifuged, and the clear supernatant was collected. The product was then extracted in chloroform and characterized by ¹H NMR spectroscopy. It was found that from such a mixture only fluorene was extracted, and furthermore, the product contained exclusively fluorenone and no 2,7-dibromofluorene or 2,7-dibromofluorenone was present (Fig. S44). This strategy was then extended to a 2-bromofluorene and 2,7-dibromofluorene mixture. In this case as well, the product obtained contained selectively only 2-bromofluorenone and no 2,7-dibromofluorene or 2,7-dibromofluorenone was present (Fig. S46).

To better understand the mechanism behind this selective oxidation through selective encapsulation, firstly selective encapsulation experiments were performed. It was found that from a mixture of fluorene and 2,7-dibromofluorene, cage **1** selectively encapsulated only fluorene (Fig. S42). Similarly, from a mixture of 2-bromofluorene and 2,7-dibromofluorene, only 2-bromofluorene was encapsulated by **1** (Fig. S43). To better realize this, the K_a values for the formation of the host–guest

Fig. 5 (a) Schematic representation for the formation of octahedral cage **2** and double-square cage **3**, (b) partial ¹H NMR plot of the product obtained from **1**, (c) **2**, and (d) **3**, and (e) partial ¹H NMR plot of the xanthene. Peaks for the internal standard (1,3,5-trimethoxybenzene) are highlighted in green.
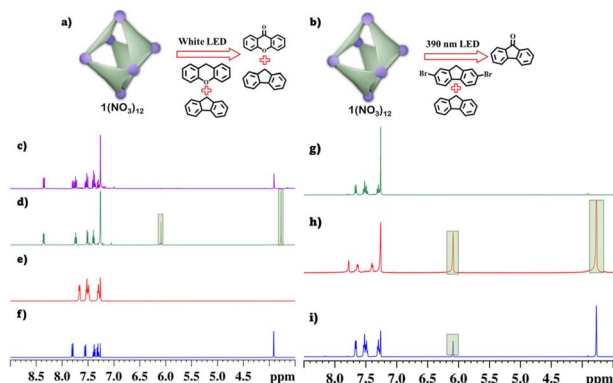
Fig. 7 Schematic diagram of the selective oxidation of (a) xanthene and (b) fluorene. ^{1}H NMR (in CDCl$_3$) stack plot of the (c) extracted product (purple plot) from the above-mentioned reaction (a). (d) Xanthone (green) in CDCl$_3$, (e) fluorenone (red) in CDCl$_3$, and (f) fluorene (blue) in CDCl$_3$, at 298 K. ^{1}H NMR stack plot of the (g) extracted product (fluorenone, green) from the above-mentioned reaction (b). (h) 2,7-Dibromofluorenone (red) in CDCl$_3$ and (i) fluorenone (blue) in CDCl$_3$ at 298 K. Peaks for the internal standard (1,3,5-trimethoxybenzene) are highlighted in green.

complexes were then calculated using UV-visible titration and BindFit software. It was found that the K_a value for the host–guest complex of **1** with fluorene was 3.97×10^4 M^{-1}, the K_a value for the complex with 2-bromofluorene was 2.78×10^4 M^{-1} and the K_a value for the one with 2,7-dibromofluorene was 1.66×10^4 M^{-1} (Fig. S37–S39). This clearly showed that by leveraging the difference in binding affinity of the substrate to the host, selective oxidation could be achieved. To further verify that the selective oxidation was due to differences in binding affinity, a mixture of fluorene and 2-bromofluorene was selected, as they have very similar binding affinities, and it is expected that in such a case both molecules would be oxidized, but as the binding affinity for fluorene is slightly more, a greater amount of fluorenone must still be present in the mixture. The experimental observations verified this: when a mixture of fluorene and 2-bromofluorene was used, the product contained both the oxidized products in a ratio of 84 : 16 for fluorenone and 2-bromofluorenone, respectively.

Selective guest encapsulation experiments also showed similar results and from a mixture of fluorene and 2-bromofluorene, cage **1** encapsulated both molecules in a ratio of ∼84 : 16, which closely collaborated with the ratio of oxidized products. This clearly established that binding affinity played a major role in determining the relative selectivity of oxidation.

Conclusion

In summary, we have demonstrated a strategy for the selective oxidation of benzylic C(sp^3)–H by leveraging the selective binding affinity of a water-soluble Pd$_6$L$_4$ octahedral cage **1**. **1** was synthesized in high yield through the metal–ligand coordination-driven self-assembly of the acceptor *cis*-[(en) Pd(NO$_3$)$_2$] (**A**) with the donor **L** [2,4,6-tri(pyridine-4-yl) pyrimidine] in a 3 : 2 molar ratio. The cage **1** had an

octahedral structure with a large interior hydrophobic cavity. **1** encapsulated a variety of organic molecules like xanthene, fluorene, thioxanthene, and acridine derivatives. Further, it was found that xanthene (**X**) encapsulated inside **1** was oxidized to xanthone (**XO**) when stirred under white light for 10 hours at 50 °C in air. This transformation was investigated with previously synthesized Pd$_6$L$_4$ cages **2** (with an octahedral structure) and cage **3** (with a double-square structure). Under similar conditions, cages **2** and **3** enabled incomplete oxidation of xanthene, and reaction rate monitoring showed that the reaction inside cage **1** was much faster than reactions inside other known Pd$_6$L$_4$ cages (**2** and **3**). Further, it was found that host–guest complex formation was pivotal for the oxidation of the substrate to occur in aqueous medium. As encapsulation was pivotal for oxidation, the selective host–guest complex formation ability of cage **1** could be further utilized for selective oxidation through selective encapsulation. Utilizing this approach, from a mixture of 2,7-dibromofluorene and fluorene, fluorene could be selectively oxidized. Similarly, from a mixture of 2,7-dibromofluorene and 2-bromofluorene, selectively only 2-bromofluorene could be oxidized. The selective host–guest binding ability of the cage could also be utilized for the selective oxidation of fluorene over 2-bromofluorene with a selectivity of 84%. We envision that this strategy can be used further in other chemical transformations to achieve selectivity in chemical transformations observed in confined cavities.

Author contributions

D. C. and S. A. designed the project and the experiments. S. A. and D. C. carried out the experimental work, analyzed the data, and optimized the structures. P. S. M. supervised the project. All the authors contributed to the writing of the manuscript.

Conflicts of interest

There are no conflicts to declare.

Data availability

All data are provided in the SI and additional data can be available upon request.

NMR spectra, ESI-MS, optimized structures, and experimental details. See DOI: **https://doi.org/10.1039/d5sc02078f**.

Acknowledgements

References

1 A. Küchler, M. Yoshimoto, S. Luginbühl, F. Mavelli and P. Walde, *Nat. Nanotechnol.*, 2016, **11**, 409–420.

2 W. Xue, E. Benchimol, A. Walther, N. Ouyang, J. J. Holstein, T. K. Ronson, J. Openy, Y. Zhou, K. Wu and R. Chowdhury, *J. Am. Chem. Soc.*, 2024, **146**, 32730–32737.

3 M. Hall and A. S. Bommarius, *Chem. Rev.*, 2011, **111**, 4088–4110.

4 J. A. Davies, T. K. Ronson and J. R. Nitschke, *J. Am. Chem. Soc.*, 2024, **146**, 5215–5223.

5 V. Marcos, A. J. Stephens, J. Jaramillo-Garcia, A. L. Nussbaumer, S. L. Woltering, A. Valero, J.-F. Lemonnier, I. J. Vitorica-Yrezabal and D. A. Leigh, *Science*, 2016, **352**, 1555–1559.

6 Z. Zhang, L. Ma, F. Fang, Y. Hou, C. Lu, C. Mu, Y. Zhang, H. Liu, K. Gao and M. Wang, *JACS Au*, 2022, **2**, 1479–1487.

7 H. Tang, H.-N. Zhang, X. Gao, Y. Zou and G.-X. Jin, *J. Am. Chem. Soc.*, 2024, **146**, 16020–16027.

8 P. Liu, F. Fang, L. O. Alimi, B. A. Moosa, X. Zhu, X. Liu, H. Wang and N. M. Khashab, *Chem*, 2024, **10**, 3184–3198.

9 X.-Q. Guo, P. Yu, L.-P. Zhou, S.-J. Hu, X.-F. Duan, L.-X. Cai, L. Bao, X. Lu and Q.-F. Sun, *Nature Synthesis*, 2025, 1–11.

10 E. Benchimol, I. Regeni, B. Zhang, M. Kabiri, J. J. Holstein and G. H. Clever, *J. Am. Chem. Soc.*, 2024, **146**, 6905–6911.

11 P. Molinska, A. Tarzia, L. Male, K. E. Jelfs and J. E. Lewis, *Angew. Chem., Int. Ed.*, 2023, **135**, e202315451.

12 D. Zhang, L. Wang, W. Wu, D. Cao and H. Tang, *Chem. Commun.*, 2025, **61**, 599–611.

13 P. Suating, L. B. Kimberly, M. B. Ewe, S. L. Chang, J. M. Fontenot, P. R. Sultane, C. W. Bielawski, D. A. Decato, O. B. Berryman and A. B. Taylor, *J. Am. Chem. Soc.*, 2024, **146**, 7649–7657.

14 H. Wu, Y. Wang, L. Đorđević, P. Kundu, S. Bhunia, A. X.-Y. Chen, L. Feng, D. Shen, W. Liu and L. Zhang, *Nature*, 2025, **637**, 347–353.

15 M. Fujita, D. Oguro, M. Miyazawa, H. Oka, K. Yamaguchi and K. Ogura, *Nature*, 1995, **378**, 469–471.

16 D. Chakraborty, N. Kaur, J. Sahoo, N. Hickey, M. De and P. S. Mukherjee, *J. Am. Chem. Soc.*, 2024, **146**, 24901–24910.

17 D. M. Dalton, S. R. Ellis, E. M. Nichols, R. A. Mathies, F. D. Toste, R. G. Bergman and K. N. Raymond, *J. Am. Chem. Soc.*, 2015, **137**, 10128–10131.

18 Q. N. N. Nguyen, K. T. Xia, Y. Zhang, N. Chen, M. Morimoto, X. Pei, Y. Ha, J. Guo, W. Yang and L.-P. Wang, *J. Am. Chem. Soc.*, 2022, **144**, 11413–11424.

19 R. Banerjee, D. Chakraborty and P. S. Mukherjee, *J. Am. Chem. Soc.*, 2023, **145**, 7692–7711.

20 Y. Sun, C. Chen and P. J. Stang, *Acc. Chem. Res.*, 2019, **52**, 802–817.

21 B. Song, S. Kandapal, J. Gu, K. Zhang, A. Reese, Y. Ying, L. Wang, H. Wang, Y. Li and M. Wang, *Nat. Commun.*, 2018, **9**, 4575.

22 P. Wei, X. Yan and F. Huang, *Chem. Soc. Rev.*, 2015, **44**, 815–832.

23 L.-J. Chen and H.-B. Yang, *Acc. Chem. Res.*, 2018, **51**, 2699–2710.

24 Y. Li, S. S. Rajasree, G. Y. Lee, J. Yu, J.-H. Tang, R. Ni, G. Li, K. N. Houk, P. Deria and P. J. Stang, *J. Am. Chem. Soc.*, 2021, **143**, 2908–2919.

25 W. J. Li, X. Q. Wang, D. Y. Zhang, Y. X. Hu, W. T. Xu, L. Xu, W. Wang and H. B. Yang, *Angew. Chem., Int. Ed.*, 2021, **133**, 18909–18916.

26 H. Liu, Z. Zhang, C. Mu, L. Ma, H. Yuan, S. Ling, H. Wang, X. Li and M. Zhang, *Angew. Chem., Int. Ed.*, 2022, **61**, e202207289.

27 Z. Zhang, Z. Zhao, L. Wu, S. Lu, S. Ling, G. Li, L. Xu, L. Ma, Y. Hou and X. Wang, *J. Am. Chem. Soc.*, 2020, **142**, 2592–2600.

28 L. A. Pérez-Márquez, M. D. Perretti, R. García-Rodríguez, F. Lahoz and R. Carrillo, *Angew. Chem., Int. Ed.*, 2022, **61**, e202205403.

29 D. Chakraborty, S. Pradhan, J. K. Clegg and P. S. Mukherjee, *Inorg. Chem.*, 2024, **63**, 14924–14932.

30 A. B. Sainaba, M. Venkateswarulu, P. Bhandari, K. S. A. Arachchige, J. K. Clegg and P. S. Mukherjee, *J. Am. Chem. Soc.*, 2022, **144**, 7504–7513.

31 D. Samanta, D. Galaktionova, J. Gemen, L. J. Shimon, Y. Diskin-Posner, L. Avram, P. Král and R. Klajn, *Nat. Commun.*, 2018, **9**, 641.

32 H. Takezawa, S. Akiba, T. Murase and M. Fujita, *J. Am. Chem. Soc.*, 2015, **137**, 7043–7046.

33 Y.-F. Zhou, D.-N. Yan, S.-J. Hu, L.-P. Zhou, L.-X. Cai and Q.-F. Sun, *Dalton Trans.*, 2023, **52**, 8135–8141.

34 V. Martí-Centelles, A. L. Lawrence and P. J. Lusby, *J. Am. Chem. Soc.*, 2018, **140**, 2862–2868.

35 S. M. Bierschenk, R. G. Bergman, K. N. Raymond and F. D. Toste, *J. Am. Chem. Soc.*, 2020, **142**, 733–737.

36 M. R. Crawley, D. Zhang and T. R. Cook, *Inorg. Chem. Front.*, 2023, **10**, 316–324.

37 R. Banerjee, D. Chakraborty, W. T. Jhang, Y. T. Chan and P. S. Mukherjee, *Angew. Chem., Int. Ed.*, 2023, **62**, e202305338.

38 H. Takezawa, Y. Fujii, T. Murase and M. Fujita, *Angew. Chem., Int. Ed.*, 2022, **134**, e202203970.

39 T. Hong, Z. Zhang, Y. Sun, J.-J. Tao, J.-D. Tang, C. Xie, M. Wang, F. Chen, S.-S. Xie and S. Li, *J. Am. Chem. Soc.*, 2020, **142**, 10244–10249.

40 D. Roy, S. Paul and J. Dasgupta, *Angew. Chem., Int. Ed.*, 2023, **135**, e202312500.

41 N. Li, Q. Wang, S. Zhuo and L.-P. Xu, *ACS Catal.*, 2023, **13**, 10531–10540.

42 D.-H. Qu, Q.-C. Wang, Q.-W. Zhang, X. Ma and H. Tian, *Chem. Rev.*, 2015, **115**, 7543–7588.

43 J. R. Bourne, *Org. Process Res. Dev.*, 2003, **7**, 471–508.

44 E. Lindbäck, S. Dawaigher and K. Wärnmark, *Chem.–Eur. J.*, 2014, **20**, 13432–13481.

45 R. G. DiNardi, S. Rasheed, S. S. Capomolla, M. H. Chak, I. A. Middleton, L. K. Macreadie, J. P. Violi, W. A. Donald, P. J. Lusby and J. E. Beves, *J. Am. Chem. Soc.*, 2024, **146**, 21196–21202.

46 D. Chakraborty, S. Ali, P. Choudhury, N. Hickey and P. S. Mukherjee, *J. Am. Chem. Soc.*, 2023, **145**, 26973–26982.

47 G. R. Genov, H. Takezawa, H. Hayakawa and M. Fujita, *J. Am. Chem. Soc.*, 2023, **145**, 17013–17017.

48 M. Yoshizawa, M. Tamura and M. Fujita, *Science*, 2006, **312**, 251–254.

49 B. M. Sahoo, M. Rajeswari, P. Jnyanaranjan and S. Binayani, *Indian J. Pharm. Educ. Res.*, 2017, **51**, S700–S706.

50 D. Samanta, S. Mukherjee, Y. P. Patil and P. S. Mukherjee, *Chem.–Eur. J.*, 2012, **18**, 12322–12329.

51 T. Murase, Y. Nishijima and M. Fujita, *J. Am. Chem. Soc.*, 2012, **134**, 162–164.

52 V. Martí-Centelles, A. L. Lawrence and P. J. Lusby, *J. Am. Chem. Soc.*, 2018, **140**, 2862–2868.

53 J.-N. Chen, X.-K. Wu, C.-H. Lu and X. Li, *Biochem. Biophys. Res. Commun.*, 2019, **513**, 313–318.

54 J. Liu, H. Bao, H. Wang, Q. Luo, J. Zuo, Z. Liu, S. Qiu, X. Sun and X. Liu, *RSC Adv.*, 2019, **9**, 40781–40791.

55 F.-a. Liu, X. Lin, X. Zhou, M. Chen, X. Huang, B. Yang and H. Tao, *Molecules*, 2017, **22**, 1999.

56 R. Prebil, G. Stavber and S. Stavber, *Eur. J. Org Chem.*, 2014, **2014**, 395–402.

57 H. Kawabata and M. Hayashi, *Tetrahedron Lett.*, 2004, **45**, 5457–5459.

58 X. Zhao, X. Zheng, B. Yang, J. Sheng and K. Lu, *Org. Biomol. Chem.*, 2018, **16**, 1200–1204.

59 K. Bahrami, M. M. Khodaei and A. Farrokhi, *Tetrahedron*, 2009, **65**, 7658–7661.

60 A. Stankiewicz-Drogon, L. G. Palchykovska, V. G. Kostina, I. V. Alexeeva, A. D. Shved and A. M. Boguszewska-Chachulska, *Bioorg. Med. Chem.*, 2008, **16**, 8846–8852.

61 R. M. Ngoumfo, J.-B. Jouda, F. T. Mouafo, J. Komguem, C. D. Mbazoa, T. C. Shiao, M. I. Choudhary, H. Laatsch, J. Legault and A. Pichette, *Bioorg. Med. Chem.*, 2010, **18**, 3601–3605.

62 J. Zhou, M. Li, T. Li, C. Li, X. Hu, L. Jin, N. Sun, B. Hu and Z. Shen, *Tetrahedron*, 2021, **82**, 131947.

63 A. Das, I. Mandal, R. Venkatramani and J. Dasgupta, *Sci. Adv.*, 2019, **5**, eaav4806.

64 M. Yoshizawa, S. Miyagi, M. Kawano, K. Ishiguro and M. Fujita, *J. Am. Chem. Soc.*, 2004, **126**, 9172–9173.

65 S. Ghosal, A. Das, D. Roy and J. Dasgupta, *Nat. Commun.*, 2024, **15**, 1810.